

Figures and text from Dittmann et al (2009a, 2009b) reproduced with permission from AAS

Observing Extrasolar Planets at the University of Arizona's Kuiper Telescope

Jason A. Dittmann

dittmann@email.arizona.edu

1. Statement of Purpose

The purpose of this honors thesis is to investigate the nature of planets around other stars by observing them as they pass in front of their parent star as seen from the Earth.

2. Statment of Relevance

Since the first discovery of a planet outside of the Solar System (Mayor et al. (1995)), more than 400 exoplanets have been discovered¹, 70 of which are transiting. As this field continues to grow, there is a need not only for searches of new planets, but of follow up studies of the ones that have been discovered. The goal of this thesis is to contribute to the knowledge about known exoplanet systems through photometric study.

3. Methodology

Data was taken at the University of Arizona's 61-inch (1.55m) Kuiper telescope on Mt Bigelow, Arizona. Data for the extrasolar planet TrES-1b was taken on 12 May 2009 and 15 May 2009 UT; data for HAT-P-11b was taken on 01 May 2009 UT.. For each observation, the Mont4k CCD was used, binned 3x3 to 0.43"/pix. An R-filter was used during observations of TrES-1b, and a Strommgen-b used for HAT-P-11b.

Before and after each observing run, several hundred dome flat images were obtained with the filter used that night, as well as several hundred bias images, to reduce the error

¹Steward Observatory, University of Arizona, Tucson, AZ 85721

¹exoplanet.eu

budget in the data. The time stamp for each image is written by the clock on the CCD computer, which is synchronized with the on-site GPS system every 2 minutes, so that the time is always correct to within a couple tenths of a second.

On 12 May 2008 weather conditions were slightly cloudy with less than 1 magnitude extinction. For all other observing nights, conditions were photometric. All images from each observing run were bias subtracted, flat field corrected, and bad pixel cleaned in the usual manner using standard IRAF² tasks. Additional data reduction tasks done for specific objects will be explained under the following subsections for each individual object.

3.1. TrES-1b

Photometry and photometric errors were obtained on all images using the DAOPHOT package in IRAF. Relative photometry was done using reference stars in the field of view. The reference stars were normalized to unity and then weighted according to their average fluxes. We applied 2σ clipping to the reference stars. However, data points for TrES-1 were not clipped. On 15 May 2009, four reference stars were used, while only two of those four were used on May 12 since, due to the patchiness of clouds, we were forced to use only the reference stars that were closest to TrES-1. Our final data for TrES-1 has a photometric RMS range of $\sim 1 - 2$ mmag and a time sampling of ~ 40 seconds, typical of the precision achieved with the Mont4k on the 61" telescope for high S/N images (Randall et al. (2007), Dittmann et al. (2009a)).

Each of the planetary transit light curves were fit using the χ^2 method prescribed by Mandel and Agol (2002). The transit parameters used in the fit were compiled by Butler et al. (2006) from Alonso et al. (2004), while the impact parameter was provided by Gaudi and Winn (2007). Linear and quadratic limb darkening parameters were taken from Claret (2000). In order to understand and characterize departures from the transit related to starspot occultation, the only parameter that was allowed to vary in the fit was the central time of each transit, T_c .

²IRAF is distributed by the National Optical Astronomy Observatories, which are operated by the Associate of Universities for Research in Astronomy, Inc., under cooperative agreement with the National Science Foundation.

3.2. HAT-P-11

HAT-P-11 is a challenging object to observe, since the transit depth is only ~ 4.3 mmag (0.43%), and is a very bright K4 star ($V=9.6$) with a nearby faint (likely background) star. Defocusing the telescope to obtain larger exposure times was not possible, as HAT-P-11 is in the crowded Kepler field. Furthermore, all possible reference stars are several magnitudes fainter than HAT-P-11 itself. In order to take long enough exposures to sufficiently average out atmospheric scintillation while avoiding saturating the CCD, we used a medium bandwidth Stromgren b filter ($\Delta\lambda = 18.0$ nm). The Mont4k filter holder and filter sensor position were specifically modified to accommodate the thicker Stromgren filter for our observations. With this setup, we were able to use an exposure time of 17s and a sampling of 28.3 s for the transit observations.

Photometry and photometric errors were obtained on all images using the DAOPHOT package in IRAF. Relative photometry was done using reference stars in the field of view. The final light curve for HAT-P-11 was normalized by division of the weighted average of the three reference stars. We applied no sigma clipping rejection to any of our data points. Our final data for HAT-P-11 has a photometric RMS of 1.7 mmag, typical of the precision achieved with the Mont4k on the 61" telescope for high S/N images (Randall et al. (2007), Dittmann et al. (2009a and b)).

The transit light curve was fit using the χ^2 method of Mandel and Agol (2002). The transit parameters used in the fit were those measured by Bakos et al. (2009), while the linear and quadratic limb darkening coefficients were taken from Claret (2000). The only parameter allowed to vary in the fit was the central time of transit T_c , as the purpose of these observations was not to re-derive all the parameters of the transit, but to understand if our transit is consistent with the period of Bakos et al. (2009).

4. Literature Review

The transit of an extrasolar planet across the face of its host star allows direct measurements of the bulk properties of the planet. In particular, the transit allows accurate measurement of the planet's radius (see for example Charbonneau et al. 2006 and references therein). Combined with the radial velocity (RV) measurements of masses, then densities of the transiting planet can be calculated. Furthermore, knowledge of the heating from the star allows estimates of the temperatures of the irradiated planets. Models of the bulk properties of these planets can be compared to observation (see for example Baraffe et al. 2008; Fortney et al. 2007; Burrows et al. 2007; Seager et al. 2007).

While this method is good for detecting planets, and can provide excellent characterization of the system, it requires very precise alignment of the planet’s orbit relative to the line of sight from Earth, and thus only a small portion of discovered planets are transiting. Furthermore, the sensitivity to very low radii, and hence masses, is limited. While facilities such as the Kepler Space Telescope may soon be able to detect planets as small or smaller than Earth (Borucki et al. 2008), there are currently only three known extrasolar transit planets as small as or smaller than Neptune in mass: GJ 436b with a mass of $\sim 21M_{\oplus}$ (Butler et al. 2004), HAT-P-11b with a mass of $\sim 25M_{\oplus}$ (Bakos et al. 2009), and the recently discovered CoRoT-7b with a mass of $\sim 11M_{\oplus}$ (Rouan et al. 2009).

While this limitation is discouraging, it is far from absolute. It was shown by Mirlada-Escude (2002) that even a relatively small secondary planet in a multiple planet system can induce significant observable changes in the orbital parameters of the transiting planet. Most notably in the duration of the transit, the timing of the transit, and the inclination angle. Grazing or near-grazing transits are especially sensitive to this type of perturbation (Ribas et al. (2008)). Several systems have been thoroughly examined for these types of perturbations, and in the case of GJ 436b there have been no positive signs (Ribas et al. 2008; Alonso et al. 2008; Bean et al. 2008). It is a search for deviations from the standard transit light curves that motivated the research presented here. In specific, deviations related to starspot occultation were investigated for TrES-1b, and searches for transit timing variations motivated the observations of HAT-P-11b. More detailed information about each of these systems are presented in the following subsections.

4.1. The TrES-1 System

TrES-1b is a Jupiter sized extrasolar planet orbiting a 12th magnitude K0V star, discovered by Alonso et al. (2004) using the transit search method. Since then, there have been numerous investigations regarding photometric anomalies during transits of TrES-1b. Hubble Space Telescope ACS spectra analyzed in Rabus et al. (2009) show a very significant ($\sim 2.7 \pm 0.2$ mmag) brightening anomaly just before the center of transit. Professional and amateur data taken and compiled by Price et al. (2006) show a ~ 5 mmag brightening even during the egress of the transit. Studying of anomalies just outside of egress led to the suggestion of trojan-like objects, which have been constrained by Ford and Gaudi (2006).

In order to understand the strange anomalies inside the transit light curve, Winn et al. (2007) obtained transit light curves in the far red z-band for three consecutive transits of TrES-1b with the FWLO 1.2 m and KeplerCam. Their light curves had low scatter, ~ 1 mmag, and they found no evidence for the existence of anomalies either inside or outside

of the transit over a 9 day period. However, if those anomalies were caused by the planet transiting in front of a starspot, then observations in the z-filter used by Winn et al. (2007) would be much less sensitive to starspots than the bluer filters used in the previous studies (or there were no spots visible over those 9 days). Rabus et al. (2009) show in their HST ACS spectral data that their anomaly is sensitive to wavelength with a peak in the $H\alpha$ bin (as expected for a cool starspot, and as demonstrated in a similar study by Pont et al. (2007)), though they argue this peak might not be real due to higher noise in that wavelength bin. However, they do find that the brightening event is smaller for longer wavelengths, suggesting that Winn et al. (2007)’s z-band data may not have been sensitive to such spots on TrES-1.

Rabus et al. (2009) present two possible explanations for these anomalies; starspots, or the first double transiting planetary system. They argue that a starspot crossing event would be wavelength dependent while a double transit would not. Also, starspots on the star would appear in different locations from transit to transit, while a planet-planet occultation would be a very rare event unless the planets were in a resonant orbit. Rabus et al. (2009) also modeled a double planet transit to simulate their data and were able to create a lower bound on the radius of the second planet of $1.081 R_J$. They argue that more observations are required to definitively understand the nature of the HST anomaly.

Our own group observed a very similar anomaly to that of Rabus et al. (2009) in April 2007 in the R band. This prompted up follow-up observations in the following here. We have shown in Dittmann et al. (2009b) that these brightening anomalies are indeed spots.

4.2. The HAT-P-11 System

HAT-P-11b is the second transiting Neptune ever discovered, in orbit around HAT-P-11 (2MASS 19505021+4804508), a K4 ($V=9.6$ mag) metal rich star. This planet was discovered by the hATNet array of small 0.11m telescopes on Mt. Hopkins in Arizona (Bakos et al. (2009)). At just 4.2 mmag, HAT-P-11b was the smallest planet discovered by the transit method.

Detailed RV measurements by Bakos et al. (2009) show a linear drift (0.0297 ± 0.0050 m/s/day) in the RV residual of HAT-P-11. This drift is possibly due to the pull of an unseen planet in the system (Bakos et al. (2009)). In addition, Bakos et al. (2009) determine a nonzero (0.198 ± 0.046) eccentricity which might be maintained by interactions with another planet. Both observations hint at the presence of another outer planet "HAT-P-11c" in the system. Indeed, most systems with super Neptunes are multiple planet systems (Bakos et al. 2009 and reference within. Continued RV monitoring of this system may directly detect

curvature in the RV residuals due to this outer planet. Another way to directly detect the presence of a possible "HAT-P-11c" would be a sensitive search for transit timing variations over a series of HAT-P-11b transits. A search to bound the magnitude of such timing variations motivated our research into this object.

5. Results/Analysis

5.1. TrES-1b

On April 14, 2007 UT, a transit of TrES-1b was observed at the University of Arizona's Kuiper telescope. The data showed a brightening just before the center of the transit similar to that in Rabus et al. (2009) (see Figure 1). We found the peak of the brightening to be ~ 2.3 mmag. Since this was similar in amplitude and duration to the HST anomaly of Rabus et al. (2009), this motivated follow-up observations during May 2008. Furthermore, if the anomaly is indeed caused by a starspot, as suggested for the HST event, then the anomaly may appear later in phase in consecutive transits, and make it theoretically possible to measure the rotation rate of the star, as recently outlined in Silva-Valio (2008). Studies measuring the Rossiter-McLaughlin effect measure the tilt of the stellar rotational axis with respect to the planetary orbital axis in the plane of the sky. This effect was measured by Narita et al. (2007) for TrES-1 who found $\lambda = 30 \pm 21^\circ$. Laughlin et al. (2005) found $V_* \sin(i_*) = 1.08 \pm 0.3 \text{ km/s}$, which can also be used to constrain the rotation rate of the star.

Our transit light curves for May 2008 are shown in Figure 2. There is a 5.4 ± 1.7 mmag brightening anomaly during the first half of the transit on May 12, and one in the second half of the transit on May 15. Assuming that these anomalies are real³ and due to the occultation of a starspot or starspot group by TrES-1b, we are able to estimate the rotational period of the star. We will use the following notation:

1. I is the inclination of the stellar spin axis out of the plane of the sky ($i_* = 90 - I$).
2. λ is the sky-projected angle between the stellar spin axis and the planetary orbital axis, where we have made the good approximation that the planetary orbital axis is in the plane of the sky.

³For a full analysis of the probability of these anomalies being noise, see Dittmann et al. (2009b).

The $\lambda = 0^\circ$, $I = 0^\circ$, $i_ = 90^\circ$ Case*

We first examine the simpler case where the axes are aligned, and that the inclination of both axes along the line of site is effectively 90° (in the plane of the sky).

The geometry of this case is illustrated in Figure 3. Here, R is the radius of the circular cross-section at the transit latitude and is given by $R = R_* \cos(\text{lat})$, where the latitude is calculated from the impact parameter. For TrES-1, this yields $R = 0.984R_*$. The time of the peak of the anomaly during the transit is directly related to the projected location of the spot on the surface of the star, which can then be used to calculate the angle from the apparent central line of longitude from Earth. This is shown in figure 3. If we assume that the planet’s orbital axis and TrES-1’s spin axis are perfectly aligned in the plane of the sky ($\lambda = 0 \pm 0^\circ$), we can calculate the rotational period of the star at that latitude as:

$$P_{rot} = \frac{2\pi(T_{anomaly_2} - T_{anomaly_1})}{\theta_2 + \theta_1} \text{ Case: } \lambda = 0, I = 0 \quad (1)$$

where:

$$\theta_i = \sin^{-1} \left(2 \left[1 + \frac{R_p}{R_* \cos(\text{lat})} \right] \left[\frac{|T_{anomaly,i} - T_c|}{T_{transit}} \right] \right) \text{ rad} \quad (2)$$

Here, the factor of $\frac{R_p}{R_* \cos(\text{lat})}$ corrects for the fact that ingress is when the leading limb of the planet crosses the star and egress is when the trailing limb of the planet leaves the star. In other words, the distance traveled in the transit time ($T_{transit} = 0.115$ days or 2.76 hours for TrES-1b) is the time required to move $2R_p + 2R_* \cos(\text{lat})$ (see Figure 3).

After fitting with the method of Mandel and Agol (2002), we obtained an initial reduced χ^2 of 0.88 for May 12 and 0.97 for May 15. The χ^2 was minimized, and T_c measured, excluding the starspot anomaly points for the fit. See Table 1 for the determined transit center T_c values, as well as other system parameters.

In order to characterize the range of stellar rotation rates that we are sensitive to, we find the maximum rotation rate that TrES-1 could have in order for the starspot seen on the first night to completely rotate off the visible side of the star for the observations on May 15. In other words, $\theta_2 = 90^\circ$, and the rotational axis is in the plane of the sky so that the spot moves the maximum distance between transits. We find that the star would need to be rotating once every 10.03 days in order for this to occur. Consequently, we are then sensitive to periods > 10 days.

Using equations 1 and 2, which assume that the rotational axis of the star is in the plane

of the sky, we find a rotation rate for TrES-1 of 40.2 ± 0.1 days ($\lambda = 0 \pm 0^\circ$). Alternatively, it is possible that this star rotated through any number of whole rotations plus the observed angle change observed. If the star had completed one additional rotation between the times of observation, this would correspond to a rotation rate of 2.84 days, which we consider to be very unlikely for an old K0V star and is inconsistent with other periods measured for this system.

The $\lambda = 30 \pm 21^\circ$, $I = 0^\circ$, $i_ = 90^\circ$ Case*

It has been estimated by Narita et al. (2007) that the rotational axis and the orbital axis of the planet TrES-1b are possible misaligned. They have estimated that the sky projected angle between the orbital axis of TrES-1b and the spin axis of TrES-1, λ is $30 \pm 21^\circ$ (see Figure 4). Now our time stamp measurements of each starspot occultation lie along the transit path while the starspot itself travels a shorter path. Therefore, the true longitudinal change differs from the $\lambda = 0$, $I = 0$ case by a factor of $\sim \cos(\lambda)$. Replacing $\theta_2 + \theta_1$ in equation 1 with $(\theta_2 + \theta_1)\cos(\lambda)$ yields:

$$P_{rot} \approx \frac{2\pi(T_{anomaly_2} - T_{anomaly_1})}{(\theta_2 + \theta_1)\cos(\lambda)} \quad \lambda = 30 \pm 21^\circ, I = 0 \quad (3)$$

Using the values for λ from Narita et al. (2007), we find a period of $46.4^{+23.6}_{-0.5}$ days. Since in this case, $I = 0$, Laughlin et al. (2005)'s value of $V_* \sin(i_*) = 1.08 \pm 0.3$ km/s becomes $V_* = 1.08 \pm 0.3$ km/s because the rotational axis is in the plane of the sky (or $i_* = 90^\circ$). This yields an observed period of the star of $P_{obs} = 38.4^{+12.7}_{-8.4}$ days. Our value is slower, but still consistent with this observed period.

The $\lambda = 0^\circ$, $I = 30 \pm 21^\circ$, $i_ = 60 \pm 21^\circ$ Case*

We now move on to the case where $\lambda = 0$ but the inclination of the stellar rotation axis out of the plane of the sky is nonzero. While we have no prior constraints on this angle, I , we will make the assumption that it is the same order as Narita et al. (2007)'s measurement of λ , namely $30 \pm 21^\circ$.

In the non-zero I case, the rotational axis of the star is at a projected vertical position of $R_* \cos(I)$. When connected with the positions of the starspots, this forms a triangle, where the subtended angle is now larger than for the $I = 0$ approximation. The x_i value can still be taken from the time-stamp of the occultation by the planet (see eqn 2), but the longitudinal angle of the starspot increases so $\theta_2 + \theta_1 \sim (\theta_2 + \theta_1)/\cos(I)$. Then, the period becomes

$$P_{rot} \approx \frac{2\pi \cos(I)(T_{anomaly_2} - T_{anomaly_1})}{\theta_2 + \theta_1} \quad \lambda = 0, I = 30 \pm 21^\circ \quad (4)$$

Assuming $I = 30 \pm 21^\circ$ and equation 4 we find a rotational period of $P_{rot} \approx 34.8_{-9.5}^{+4.9}$ days. Using this inclination for the Laughlin et al. (2005) value of $V_* \sin(i_*) = 1.08 \pm 0.3$ km/s yields a rotation rate of $P_{obs} = 33.2_{-14.3}^{+22.3}$ days, taking into account the error in $i = 90 - I$ and the error in the measurement itself. Our measured P_{rot} value is also consistent with this observed P_{obs} value.

The $\lambda = 30 \pm 21^\circ, I = 30 \pm 21^\circ$ Case

In general, both λ and I are nonzero. Increasing λ tends to result in a lengthening of the period while Increasing I tends to lower the period. These two effects tend to cancel each other out if $I \sim \lambda$ and combining them yields:

$$P_{rot} \approx \frac{2\pi \cos(I)(T_{anomaly_2} - T_{anomaly_1})}{(\theta_2 + \theta_1) \cos(\lambda)} \quad \lambda = 30 \pm 21^\circ, I = 30 \pm 21^\circ \quad (5)$$

Using this, we find $P_{rot} \approx 40.2_{-14.6}^{+22.9}$ days with large uncertainties.

5.1.1. *Could These Consecutive Anomalies Be Due to a Double Transiting Planet?*

Rabus et al. (2009) postulated that the in-transit anomaly of TrES-1b they observed with HST could be due to another transiting planet in the system, and the brightening effect due to TrES-1b partially passing behind the secondary planet in our line of sight. Assuming this "double eclipse" theory is correct and that both of our events were also caused by such double eclipses requires that the outer planet, "TrES-1c" in 3.05 days covers just $0.464 R_*$ laterally, while TrES-1b only requires 0.115 days to cover $2.26 R_*$. This suggests that TrES-1c only has an orbital velocity of ~ 1.1 km/s and a semi major axis of ~ 745 AU and an orbital period of ~ 21000 years. It is clearly impossible to have such a system also produce the brightening event observed by Rabus et al. (2009) in 2004. This means that if this was a double transiting system, the TrES-1c orbital velocity required to explain the pair of 2008 events would be too slow to explain the appearance of the prior HST brightening event.

It is also possible that one of our events could be due to "TrES-1c" while the other due to a starspot occultation. However, to have these two unrelated events happen in consecutive transits at a separation completely consistent with the rotation rate of the star

is very unlikely. Therefore, we find that the most likely explanation for all of the anomaly observations to date is that TrES-1b often occults a large starspot(s) on the surface of TrES-1.

We assumed in calculating the $P_{rot} \approx 40.2_{-14.6}^{+22.9}$ day rotational period of the star that there was no significant spot evolution between observations. Starspot migration we consider to be irrelevant between observations since only a few tenths of a degree at most could be expected (Rodono et al. (1995), Strassmeier et al. (2003)). Even in the event of the starspot slightly evolving during those 3.05 days, it would only introduce small errors relative to the errors introduced due to the large uncertainty in λ into our calculations.

By approximating the starspot as 100% black, we can estimate the minimum size of the spot. The peak brightening was 5.4 mmag, and by dividing this by the depth of the main transit, ~ 25 mmag, we are able to estimate the size of the spot in terms of the size of the planet. We find that the spot is $\geq 6R_{\oplus}$ in radius. This is a large spot for our Sun, but could be common for TrES-1. We note that the HST observations were best fit by a similar sized spot of $6.6R_{\oplus}$ (Rabus et al. (2009)).

By looking at the residuals of the fit, we are able to estimate whether the anomalies that we have assumed to be real, are instead just white or red noise in the data. We have detected these brightening events at the 3.2σ level on May 12 and at the 2.9σ level on May 15. Other significant deviations from the transits (see Figure 2) are only significant at the 1.3 - 1.7σ level, which is 1.5σ lower. Therefore, we estimate that these events have a $\sim 9\%$ chance each of being a very strong red noise peak. Therefore, there is a significant chance this pair are the same spot, yet it is impossible to be 100% positive and it is also impossible to reobserve these events. However, the appearance of 3 new brightening anomalies in addition to that observed by HST strongly suggests large spots are not rare on the surface of TrES-1. For a full analysis into the effects of rednoise and the probability of these events being real, see Dittmann et al. (2009b).

5.2. HAT-P-11b

After fitting the planetary transit light curve with the χ^2 method of Mandel and Agol (2002) (see Methodology section above or Dittmann et al. (2009a) for details), we found a central time of transit of $T_c = 2454952.92534 \pm 0.00060$ BJD. The ± 0.00060 day 1σ uncertainty was estimated by Monte-Carlo simulations of 1000 simulated datasets with the same 1.7 mmag rms scatter of the original data (see Figure 6

To try and understand if our transit data suggest a different planetary radius for HAT-P-11b we repeated the fit in the last section using the χ^2 method prescribed by Mandel and Agol

(2002) but this time allowed the planetary radius R_p to vary along with T_c . In Figure 5 (left) we see the result of our fit (solid red line) and the residuals of this fit below. The results of our simultaneous fits yield $R_p/R_* = 0.0621 \pm 0.0011$ and $T_c = 2454952.92534 \pm 0.00060$ BJD. The $\pm 0.00111\sigma$ uncertainty in R_p/R_* was estimated by Monte-Carlo simulations of 1000 fake datasets with the same 1.7 mmag rms scatter as the original data (Figure 6).

5.2.1. *Is the Timing of the Transits Changing?*

The goal of this study was to compare our measured 01 May 2009 UT transit time to that predicted from the previously measured values. Projecting the $P = 4.8878162 \pm 0.0000071$ day period of Bakos et al. (2009) forward from their most accurate $T_c = 2454605.89132 \pm 0.00032$ transit suggests that our 01 May transit ($n = 71$ periods later) occurred $\Delta T = 80 \pm 73$ seconds sooner where $\sigma_{\Delta T}$ was calculated by $(\sigma_{T_{c1}}^2 + n\sigma_P^2 + \sigma_{T_{c2}}^2)^{1/2}$. However, the significance of this disagreement is small. Indeed, there is a $\sim 60\%$ probability that our observations are fully consistent with the timing measurements (and uncertainties) of Bakos et al. (2009). Certainly we can rule out large (greater than 200 second) timing errors at the $\sim 3\sigma$ level.

6. Conclusions

6.1. TrES-1b

During observations of two consecutive transits of TrES-1b, we found a brightening anomaly which we attributed to the planet crossing in front of a $\geq 6R_\oplus$ radius starspot. By observing the timing of TrES-1b eclipsing this spot during each transit, we can constrain the rotation rate of the star. Assuming that these are the same spot and that the spin axis of the star and orbital axis of the planet are aligned and in the plane of the sky suggests a stellar rotational period of 40.2 ± 0.1 days. Using the $\lambda = 30^\circ \pm 21^\circ$ inclination of the stellar spin axis with respect to the planetary orbital axis of Narita et al. (2007), there is much more uncertainty and we are able to constrain the rotational period of the star to $40.2^{+22.9}_{-14.6}$ days, which is consistent with the previously observed $P_{obs} = 33.2^{+22.3}_{-14.3}$ day period. We note that this is a tentative detection of consecutive star spot occultations where the events associated with the spot are $\sim 1.5\sigma$ higher in significance than red-noise peaks in the light curve. We estimate that there is a $\sim 9\%$ chance that each event is red noise and a $\sim 1\%$ chance that both events are red noise. In the future, this technique for measuring stellar rotations can be applied to any transiting system in which significant-sized star spots are eclipsed by the planets transiting path, then rotation rate can be constrained. If the inclination of the stellar

spin axis of the star is accurately known relative to the plane of the sky, this method could be a very accurate way to measure the rotational period of a star.

We have ruled out the possibility of these anomalies being a double planet occultation. If both starspot events were to be attributed to a double planet occultation, we find that the planet would have to have an orbital distance of ~ 745 AU and a period of $\sim 21,000$ years. This is incompatible with a similar occultation observed by Rabus et al. (2009) in 2004, and therefore we conclude that the starspot explanation is the most likely to describe all events and there is no second outer transiting planet, TrES-1c, in the system.

6.2. HAT-P-11b

We confirm the existence of the transiting planet HAT-P-11b. Our main conclusions from our 1.7 mmag rms (unbinned) transit observations (with the University of Arizona’s 1.55 Kuiper telescope) of the 2009 May 1 UT transit are

1. We find a central transit time of $T_c = 2454952.92534 \pm 0.00060$ BJD from a best fit to our data. We estimate that the transit occurred 80 ± 73 s sooner than previous (71 orbits in the past) measurements would have predicted (Bakos et al. 2009). Our finding is consistent with the ephemeris of Bakos et al. and rules out the presence of any large timing variation.
2. We derive a slightly larger planetary radius of $R_p = 0.452 \pm 0.020R_J$ ($5.07 \pm 0.22R_\oplus$) compared to Bakos et al.’s values of $0.422 \pm 0.020R_J$ ($5.07 \pm 0.22R_\oplus$). Our values suggest that HAT-P-11b is very close to GJ 436b in radius.

References

- Alonso, R., Brown, T., Torres, G., Latham, D., et al. 2004 ApJ 613, L153.
Alonso, R., Barbieri, M., Rabus, M., et al., 2008, A&A, 487, L5
Bakos, G. A., et al. 2009, arXiv:0901.0282
Baraffe, I., Chabrier, G., & Barman, T. 2008, A&A, 482, 315
Bean, J. L., Benedict, G. F., Charbonneau, D., et al. 2008, A&A, 486, 1039
Borucki, W., Koch, D., Basri, G., et al., 2008, Exoplanets: Detection, Formation and Dynamics, Proceedings of the International Astronomical Union, IAU Symposium, Vol. 249, 17
Burrows, A., Hubeny, I., Budaj, J., & Hubbard, W. B. 2007, ApJ, 661, 502
Butler, P., Vogt, S., Marcy, G., et al., 2004, ApJ, 617 L580
Butler, R.P., Wright, J.T., Marcy, G.W., Fischer, D.A., et al.. 2006 ApJ 646, 505.

- Charbonneau, D., Brown, T., Burrows, A., & Laughlin, G. 2007, in *Protostars and Planets V*, ed. B. Reipurth, D. Jewitt, & K. Keil (Tucson, AZ: University of Arizona Press), 701
- Claret, A. 2000, *A&A*, 363, 1081.
- Dittmann, J.A., Close, L.M., Green, E.M., Scuderi, L.J., Males, J.R. 2009a, *ApJ*, 699, L48.
- Dittmann, J.A., Close, L.M., Green, E.M. Fenwick, M. 2009b *ApJ*, 701, 756.
- Ford, E., Gaudi, B. 2006 *ApJ* 652, L137.
- Fortney, J. J., Marley, M. S., & Barnes, J. W. 2007, *ApJ*, 659, 1661
- Gaudi, B., Winn, J. 2007. *ApJ* 655, 550.
- Laughlin, G., Wolf, A., Vanmunster, T., Bodenheimer, P., et al. 2005 *ApJ*, 621, 1072.
- Mandel, K., & Agol, E. 2002, *ApJ*, 580, L171
- Mayor, M. and Queloz, D. 1995 *Nature* 378. (6555). 355
- Narita, N., Enya, K., Sato, B., Ohta, Yasuhiro et al.. 2007 *PASJ* 59, 763.
- Neter et al. *Applied Statistics*, 3rd ed. Boston : Allyn and Bacon, 1982.
- Pont, F., Moutou, C. 2007. *Transiting Extrasolar Planets Workshop ASP Conference Series*. 366, 209. (astro-ph/0702156v1)
- Pont, F., Gilliland, R.L., Moutou, C., Charbonneau, D. et al. 2007 *A&A* 476, 1347.
- Price, A., Bissinger, R., Laughlin, G., Gary, B., et al. 2004. *JAAVSO* 34. (astro-ph/0412463v1)
- Rabus, M. et al. 2009, *A&A*, 494, 391.
- Randall, S.K., Green, E.M., van Grootel, V., et al. 2007 *A&A* , 476, 1317-1329.
- Ribas, I., Font-Ribera, A., Beaulieu, J.P. 2008, *ApJ*, 677 L59
- Rodono, M., Lanza, A. F., Catalano, S. 1995. *A&A*. 301, 75.
- Rouan et al. 2009; *CoRoT International Symposium*
- Seager, S., Kuchner, M., Hier-Majumder, C. A., & Militzer, B. 2007, *ApJ*, 669, 1279
- Silva-Valio, A. 2008. *ApJ* 683. L179.
- Strassmeier, K.G., Kovari, Zs., Washuettl, A., Weber, M., Rice, J.B., Bartus, J. *Proceedings of 12th cambridge Workshop on Cool Stars, Stellar Systems, and the Sun*. 927. (<http://origins.colorado.edu/cs12/proceedings/poster/strassxx.pdf>)
- Winn, J., Holman, M., Roussanova, A. 2007 *ApJ* 657, 1098.
- Winn, J.N. 2006. *ASP Conference Series*. (astro-ph/0612744v1)

Table 1: Parameters of the TrES-1 System

Parameter & Value & Ref.	
P_{orbit}	$\& 3.030065 \pm 8 \times 10^{-6}$ days & Alonso et al. (2004)
a	$\& 0.0393 \pm 0.0011$ AU & Alonso et al. (2004)
M_p	$\& 0.75 \pm 0.07 M_{Jup}$ & Alonso et al. (2004)
R_p	$\& 1.08_{-0.04}^{+0.18} R_{Jup}$ & Alonso et al. (2004)
T_{transit}	$\& 0.115$ days & Alonso et al. (2004)
Latitude	$\& 18^\circ$ & Alonso et al. (2004)
R_p/R_*	$\& 0.130_{-0.003}^{+0.009}$ & Alonso et al. (2004)
P_{obs}	$\& 38.4_{-8.4}^{+12.7}$ days ^a & Laughlin et al. (2005)
P_{obs}	$\& 38.4_{-8.4}^{+12.7}$ days ^b & Narita et al. (2007), Laughlin et al. (2005)
P_{obs}	$\& 33.2_{-14.3}^{+22.3}$ days ^c & Narita et al. (2007), Laughlin et al. (2005)
P_{obs}	$\& 33.2_{-14.3}^{+22.3}$ days ^d & Narita et al. (2007), Laughlin et al. (2005)
$T_{\text{anomaly},1}$	$\& 2454598.80273$ JD & This work
$T_{\text{anomaly},2}$	$\& 2454601.85759$ JD & This work
θ_1	$\& 0.2783$ rad ^a & This work
θ_2	$\& 0.1990$ rad ^a & This work
T_c	April 14, 2007 & 2454204.91022 JD & This work
T_c	May 12, 2008 & 2454598.81648 JD & This work
T_c	May 15, 2008 & 2454601.84757 JD & This work
P_{rot}	$\& 40.2 \pm 0.1$ days ^a & This work
P_{rot}	$\& 46.4_{-0.5}^{+23.6}$ days ^b & This work
P_{rot}	$\& 34.8_{-9.5}^{+4.9}$ days ^c & This work
P_{rot}	$\& 40.2_{-14.6}^{+22.9}$ days ^d & This work

^aassuming $\lambda = 0 \pm 0^\circ$, $I = 0 \pm 0^\circ$, $i_* = 90^\circ$

^bassuming $\lambda = 30 \pm 21^\circ$, $I = 0 \pm 0^\circ$, $i_* = 90^\circ$

^cassuming $\lambda = 0 \pm 0^\circ$, $I = 30 \pm 21^\circ$, $i_* = 60 \pm 21^\circ$

^dassuming $\lambda = 30 \pm 21^\circ$, $I = 30 \pm 21^\circ$, $i_* = 60 \pm 21^\circ$

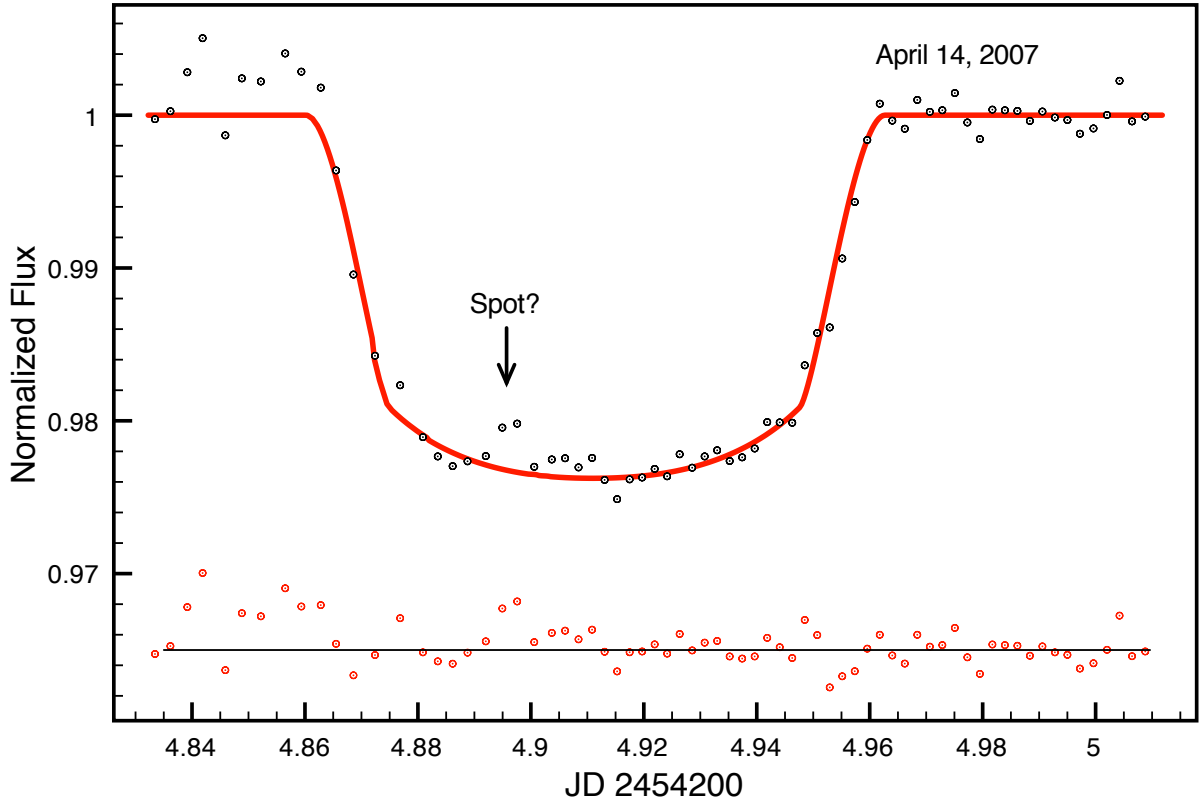


Fig. 1.— Transit light curve of TrES1-b taken on April 14, 2007 UT at the University of Arizona’s 61 inch Kuiper telescope in the R filter. Residuals of the curve from the fit are shown below. There is a tentative, ~ 2.8 mmag, brightening event just before the center of the transit. This prompted the follow-up observations of consecutive transits in 2008.

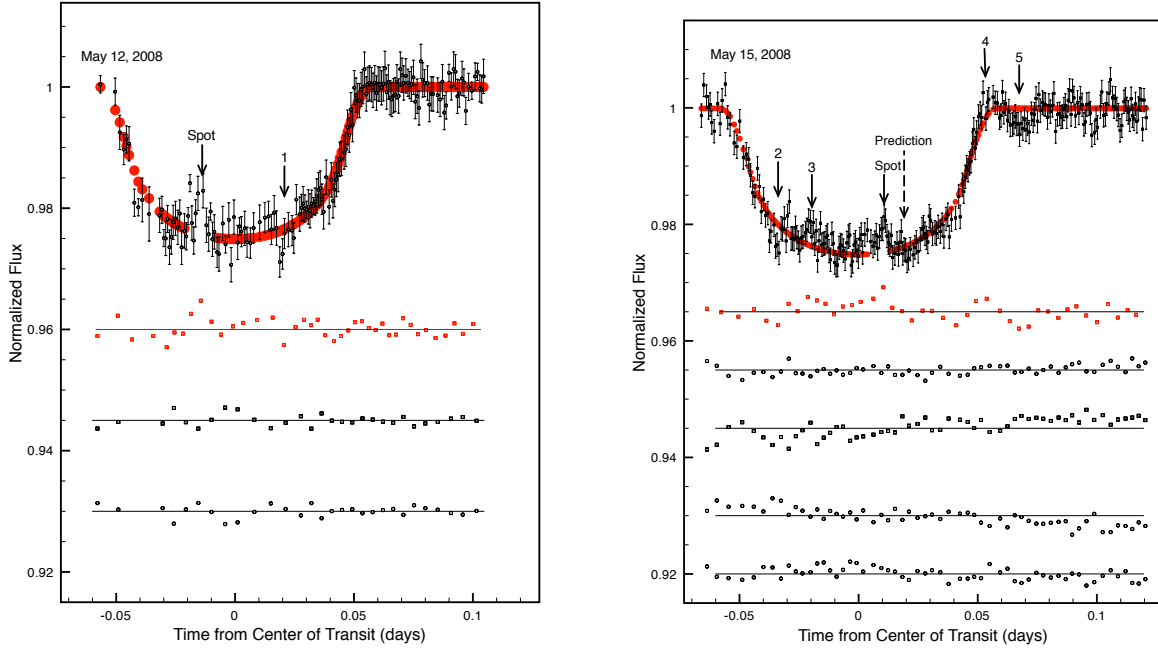


Fig. 2.— Data collected with the Mont4k CCD at the University of Arizona’s 61 inch Kuiper telescope in the R filter. The top curve is data collected on May 12, 2008 and the bottom curve is from May 15, 2008. Beneath each curve are the red data points of 5 minute discrete binned residuals of the fit. We note that we used higher (15 minute) binning just at ingress of the May 12 night due to the higher air-mass at the beginning of that observation. The anomaly is detected as a 3.2σ event on May 12 and a 2.9σ event on May 15 (see Figure ??). The predicted position of the spot on May 15 is just 27 minutes later (well within the error of P_{obs}) than actually observed (assuming the observed period of $33.2^{+22.3}_{-14.3}$ days with $I = \lambda = 30^\circ$, $V_* = 0.935$ km/s, (Narita et al. (2007), Laughlin et al. (2005))). The black points beneath each transit curve represent the reference star photometry measured for each transit.

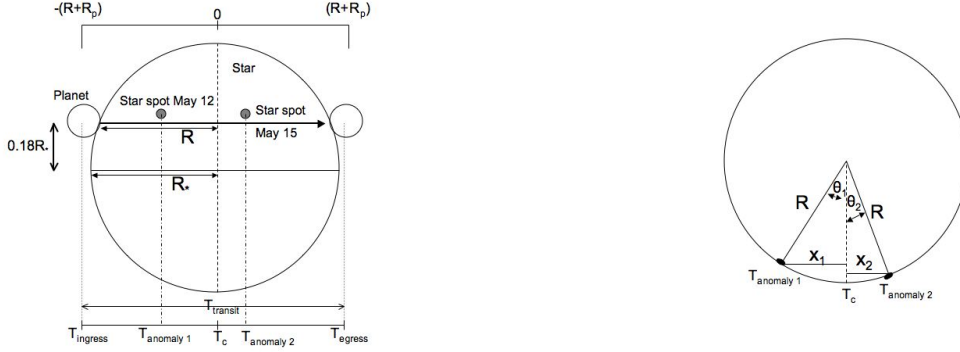


Fig. 3.— Top: Geometry of the transit ($\lambda = 0$, $I = 0$ case). The planet moves across the face of the star with an impact parameter $b = 0.18$. During each transit, it passes in front of a starspot on the face of the star. By comparing the location of the brightening event associated with the star spot during each transit, we can calculate the rotational period of the star at that latitude. Since the star is likely at an inclination of $\sim 88.4^\circ$, we assume it is exactly edge-on (90°). Bottom: Star spot location during each transit is characterized by an angle, θ . Perspective here is looking down the rotational axis of the star. $R = 0.984R_*$.

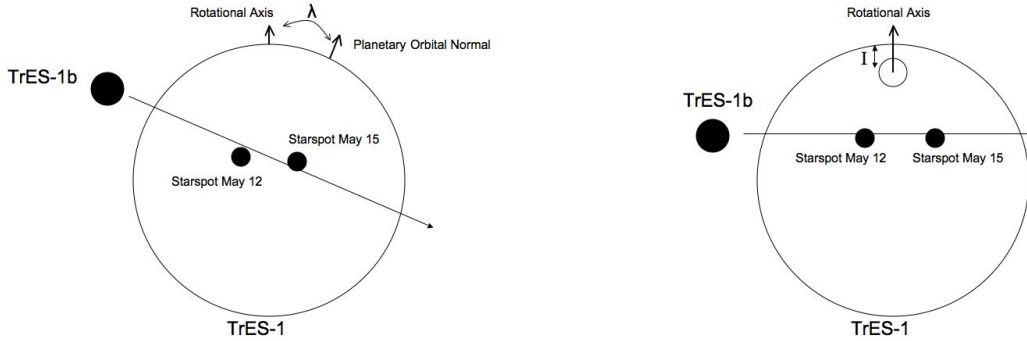


Fig. 4.— **Top**: Geometry for the nonzero λ and $I = 0^\circ$ case. While the time stamp of each starspot occultation remains the same, the longitudinal distance between them is shortened by a factor of $\cos(\lambda)$ from the $\lambda = I = 0$ case (See Figure 3). **Bottom**: Geometry for the $\lambda = 0$ and nonzero I case. Because the rotation axis of the star is tilted out of plane of the sky, the subtended longitudinal angle between starspot occultations is larger by a factor of $1/\cos(I)$ than that inferred from the time stamp alone and the $\lambda = I = 0$ geometry.

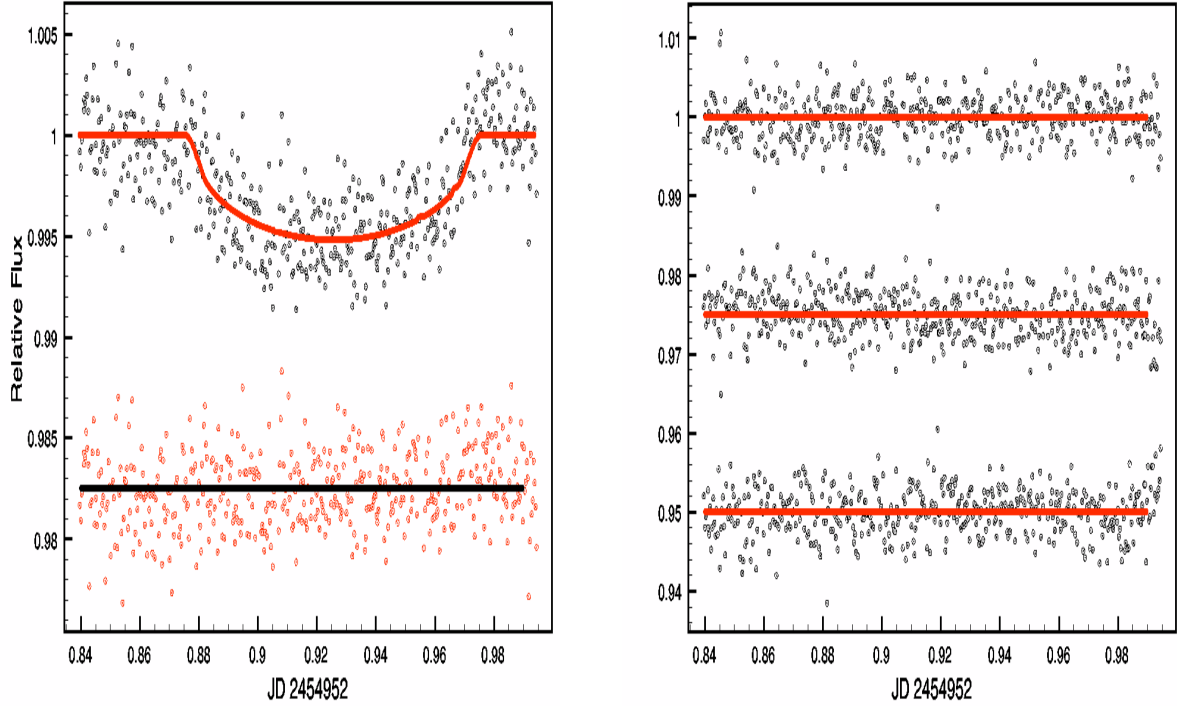


Fig. 5.— **Left:** The timeseries of HAT-P-11 during the Transit of May 1, 2009 UT. We show our best fit (reduced $\chi^2_{\nu} = 1.06$) with simultaneous fits of $R_p/R_* = 0.0621 \pm 0.0011$ and $T_c = 2454952.92534$ (solid red curve). The 1.7 mmag rms residuals of the fit are shown below. **Right:** The timeseries of our three calibrator stars (each normalized by the sum of the remaining two calibrator stars). The excellent conditions of the night allowed for mmag photometry in individual 17 or 20 second exposures even on these fainter reference stars.

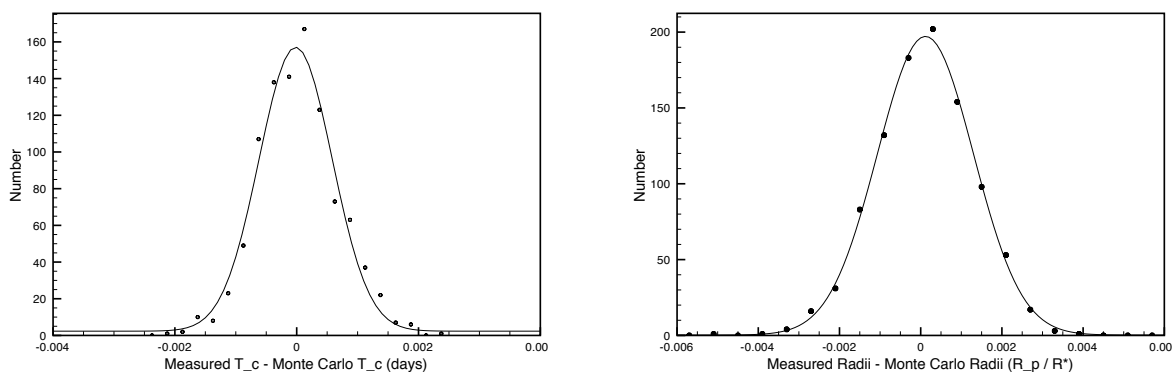


Fig. 6.— **Left:** One thousand Monte-Carlo (MC) simulations of independent simulated datasets following our best-fit transit model each drawn from a population of data with the same 1.7 mmag rms as our data in Fig. 1 (left). Based these MC simulations we find with our 1.7 mmag rms uncertainty we can constrain T_c to an accuracy of ± 0.00060 days (or 51.84 seconds) at the 1σ level. **Right:** Here another one thousand MC realizations imply the uncertainty in the R_p/R_* ratio to be ± 0.0011 at the 1σ level.